Available online at www.sciencedirect.com
SCIENCE DIRECT
Journal of Photochemistry and Photobiology A: Chemistry 176 (2005) 260–269
Journal of Photochemistry and Photobiology A:Chemistry
www.elsevier.com/locate/jphotochem

Direct measurements of the OH and NO_2 evolutions in pulsed photo-oxidation studies of hydrocarbons A method to quantify detailed and integral oxidation mechanisms in NO_x containing air

A. Hoffmann, J. Grossmann, R. Zellner *

Institute for Physical and Theoretical Chemistry, University of Duisburg-Essen, Universitätsstrasse 2, D-45141 Essen, Germany

Available online 19 October 2005

Abstract

A novel method has been developed to study the OH and NO_2 evolution in the laser pulse initiated photo-oxidation of hydrocarbons in NO_x containing gas mixtures. In this method, long-path laser absorption (LPLA) for the time resolved detection of OH radicals in the ($A^2\sum^+ - X^2\prod$) system at 308.417 nm is combined with cw-LIF for the time resolved detection of NO_2 after excitation at 488 nm at pressures around 50 mbar. It is shown that simultaneous measurements of these two species represent a detailed and sensitive signature of the elementary processes that occur following pulse initiated oxidation of hydrocarbons with photolytically generated OH radicals. The information contained in such profiles together with detailed numerical simulations permit: (i) to extract and to validate rate coefficients of otherwise difficult to access elementary processes of alkylperoxy and alkoxy radicals, (ii) to determine the extent of chain branching and OH regeneration and (iii) to derive the overall number of NO/NO_2 conversions (NOCON factors) in the complete oxidation chain of hydrocarbons. The latter are considered of substantial relevance to the assessment of individual hydrocarbons in the formation of ozone in photochemical smog mechanisms where they may be used to generate lumped oxidation schemes. The present paper describes the operation of the technique as well as the definition and derivation of NOCON factors. Because the species monitored (OH and NO_2) are not specific for any individual hydrocarbon, the technique is considered of wide applicability. A first application of the technique to the pulse initiated oxidation of propane by OH radicals at $T = 298$ K is presented.

Keywords: Pulsed photo-oxidation; Oxidation mechanism; Propane oxidation; NOCON factors

1. Introduction

Hydrocarbon oxidation is an integral part of the combustion of fossil fuels in high temperature environments. Moreover, the oxidation of volatile hydrocarbons in the atmosphere has also been identified as being an important source of ozone under NO_x containing sunlit conditions [1–3]. With the advances made in this field, it has also been shown that the oxidation chains of hydrocarbons impact on the levels of important atmospheric oxidants, such as OH radicals [4–10]. Therefore, the detailed knowledge of the mechanisms and rates of hydrocarbon oxidation is an essential pre-requisite to the understanding of such complex reactive systems.

Traditionally, the oxidation of hydrocarbons has been studied in smog chambers using the detection of the hydrocarbon loss as well as the formation of products as the objects of analysis by either GC (GC/MS) or spectroscopic (FT-IR) techniques [11–14]. Such techniques have been very valuable in generating rate constants for the initial attack of an oxidant, such as OH or NO_3 as well as in identifying product distributions [11]. With the development of more advanced techniques, i.e. pulse initiated OH generation and time resolved OH detection using resonance fluorescence [15–17], or LIF [18,19], rate constants have become available more directly. Such techniques have also been developed for some of the

* Corresponding author. Tel.: +49 201 183 3073; fax: +49 201 183 4307.
E-mail address: reinhard.zellner@uni-essen.de (R. Zellner).

1010-6030/$ – see front matter © 2005 Elsevier B.V. All rights reserved.
doi:10.1016/j.jphotochem.2005.08.011

combustion chain intermediates, such as alkoxy radicals [20–25], alkylperoxy radicals [26] and HO_2 radicals [27].

As a result of the availability of improved techniques as well as of the increased attention that this field has received over the last 2–3 decades there is now very satisfactory state of knowledge on detailed oxidation rates and mechanisms of hydrocarbons as exemplified by a number of evaluations [28–32]. This certainly applies to smaller hydrocarbons for which all elementary reactions are known with sufficient precision to model their oxidations successfully in low and high temperature environments (e.g. master chemical mechanism (MCM) [31,32]). The same, however, does not apply to larger as well as substituted or partially oxidized hydrocarbons where the number of elementary reactions increases substantially or where changes in rates and product channels are induced by substitution. Notable examples include hydroxy or halogen substituted alkoxy radicals.

One possibility to overcome the lack of direct data in the oxidation of larger and more complex hydrocarbons is the use of structure-activity-relationships (SARs). SAR approaches are now available for a number of types of reactions, including initial OH attack [33] or alkoxy [34–37] and alkylperoxy [26] radical reactions. Needless to say though that the operational quality of SAR approaches is based on the quality of available data which have been used in the development of SARs or else in the quality of theoretical ab initio quantum chemical and dynamical calculations [35–37]. Even to date there is remaining need in the provision of high quality experimental and theoretical data to be used in the further development of SARs.

Despite the need for improved detailed knowledge on oxidation mechanisms there is also a need for the reduction of such mechanisms. This is particularly the case for situations where chemistry needs to be coupled with fluid dynamics, such as in CFD modelling [38–41] or in multi-dimensional chemical-dynamical models of the atmosphere [5,9,42]. Due to computational limits these models require reductions of their chemical codes without too much loss of chemical identity. A prime example where such lumping is considered is the RADM- [43] and RACM-mechanism [44] which are used in many chemical-dynamical assessments to predict ozone levels, acid deposition, etc.

The method which has been developed and applied in this work improves on both, detailed chemical mechanisms and integrated representations. It is based on measurements of temporal evolutions of both OH and NO_2 in situations where a hydrocarbon is subjected to pulse initiated photo-oxidation in the presence of NO_x. As will be shown the technique is suitable to validate and confine existing rate coefficient of elementary oxidation reactions as well as to generate new rate coefficients with the aid of detailed model simulations. It also quantifies overall reaction mechanisms and therefore improves on currently available reduction schemes.

The present technique can be considered as a *pulsed smog chamber* technique in which in an air/hydrocarbon/NO_x atmosphere an initial oxidant (i.e. OH) is generated by pulsed laser photolysis and is monitored on the time scale of its overall decay, e.g. several ms. Simultaneously with the decay of the primary oxidant one of the oxidation products (NO_2) is also measured. Compared to a conventional smog chamber technique, the present technique operates on a compressed time scale with enhanced but measurable oxidant concentrations. The uniqueness and strength of the present technique can be summarized as follows:

1. It represents a highly sensitive method of detection of the evolution of OH and NO_2 and hence the detailed mechanisms involving HO_x and NO_x species in hydrocarbon oxidation reactions under NO_x-rich conditions. Since it is independent of the nature of the hydrocarbon it is of high applicability.
2. Due to the extremely low initial oxidant concentrations (approximately 10^{11} cm^{-3}), the monitoring of OH and NO_2 only encompasses processes which occur along the oxidation chain of the parent hydrocarbon and which proceed to the next stable product, e.g. a carbonyl compound. Subsequent reactions of carbonyl compounds can be entirely neglected.
3. It allows to determine the extent of radical recycling, i.e. the efficiency of OH regeneration in hydrocarbon chain oxidation under NO_x rich conditions.
4. It permits to define and to measure NOCON factors, i.e. the number of NO molecules converted to NO_2 per molecule of hydrocarbon oxidized. Because NO_2 is the photochemical source of ozone in the lower troposphere, this number represents the mechanistic propensity of a hydrocarbon to contribute to ozone formation. NOCON factors are substance specific but depend somewhat on the NO_x level due to the interaction of the oxidation chain with NO_x in some of the elementary processes.

2. Experimental set-up and data analysis

2.1. Laser photolysis/long-path absorption (LPLA)/LIF system

The experimental technique applied in this study is a combination of laser pulse photolysis for the direct (i.e. photolysis of alkylhalogenides) or indirect (OH or Cl attack on hydrocarbons) generation of alkyl radicals in the presence of O_2/NO and simultaneous detection of OH and NO_2 concentration–time profiles using long-path laser absorption and LIF, respectively [45–49]. From such profiles rate constants and/or branching ratios for several of the elementary reactions involved can be derived by numerical simulations using a complete chemical mechanism. Because the evolutions of OH and NO_2 have quasi-independent and different sensitivities to the individual elementary reactions, the combination of the two helps to improve the accuracy of the derived rate coefficients [48,49]. A schematic representation of the experimental set-up is shown in Fig. 1.

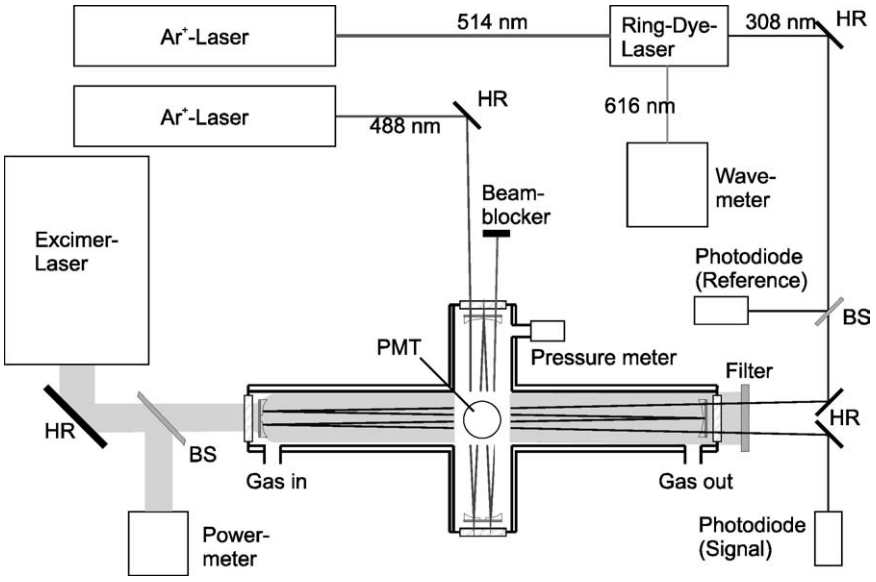

Fig. 1. Schematic representation of laser photolyis/laser long-path absorption (LPLA)/cw-LIF technique for simultaneous and time resolved detection of OH and NO_2 in the pulse initiated oxidation of hydrocarbons.

In cases such as propane, the oxidation has been initiated by OH radicals which were generated by excimer laser photolysis of H_2O_2 at 248 nm. With a typical H_2O_2 concentration of 3.0×10^{13} cm^{-3} and a typical laser fluence of approximately 30–40 mJ cm^{-2}, the initial concentration of OH radicals was estimated to be of the order of 10^{11} cm^{-3}.

The NO_2 generated in the subsequent oxidation as a result of the interaction of the oxidation intermediates (alkylperoxy and HO_2 radicals) with NO was monitored by cw-laser induced fluorescence (LIF) after excitation at 488 nm with the direct output of a 1 W Ar^+-laser. The excitation beam was coupled into a White cell to maximize the excitation volume and hence to decrease the detection limit which in this set-up was approximately 1×10^{10} cm^{-3}. After detection of the fluorescence light by a PMT, the LIF signal was further processed by a lock-in amplifier and a digital storage oscilloscope before being stored in a computer. In the quantification of the time resolved detection of small amounts of NO_2, we have encountered two difficulties: (i) we have noted the production of small amounts of background NO_2 in our gas mixture which needed to be subtracted from the overall signal monitored and (ii) the amount of NO_2 generated during the course of the oxidation chain was found to be slightly declining as a result of diffusion out of the generation volume. This effect was corrected for by applying a first-order diffusional loss constant of 4 s^{-1}.

OH radicals were detected by laser long-path absorption in the centre of the $Q_1(4)$ line of the $A^2\Sigma^+ - X^2\Pi(0, 0)$ transition at 308.417 nm. The detection wavelength has been supplied by an Ar^+-laser pumped ring-dye laser. The dye laser was equipped with an SHG unit converting the fundamental wavelength of 616 nm into the UV wavelength required for OH detection. Again mirrors in White configuration were used to maximize the detection efficiency. The typical absorption path length of 33.6 m yielded a detection limit of approximately 1×10^9 cm^{-3}. Details of this experimental arrangement have been described elsewhere [47,48,50].

The reaction mixture consisted of O_2/N_2, NO, propane and H_2O_2. The flows and hence the concentrations of all reactants were controlled by mass flow controllers. Oxygen and NO were directly taken as delivered by the manufacturer (Messer-Griesheim). A propane gas mixture was prepared by expanding 50 mbar of propane into a 20 l storage bulb and filling the bulb to a total pressure of 1000 mbar with N_2. Propane was used without further purification (Messer-Griesheim, 3.5). H_2O_2 was supplied to the gas flow using a stabilized H_2O_2/H_2O solution (60 wt.% H_2O_2, Solvay) which was saturated by a N_2 flow at 295 K and 0.5 bar overpressure. The exact H_2O_2 concentration was determined in separate experiments using the measured decay of the OH concentration in reaction with H_2O_2 itself under first order conditions.

Typical concentrations were: $[O_2] = 1.2 \times 10^{18}$ cm^{-3}, $[NO] = (0.2–1.2) \times 10^{14}$ cm^{-3}, $[propane] = 1.0 \times 10^{15}$ cm^{-3} and $[H_2O_2] = 3.0 \times 10^{13}$ cm^{-3}. All experiments have been carried out at 298 ± 3 K and a total pressure of 50 mbar. Although there is basically no constraint to use still higher pressures this value was chosen as a compromise between the needs to reproduce atmospheric conditions on the one hand and the decrease of the NO_2 detection method due to fluorescence quenching on the other hand [51].

2.2. NOCON factors: definitions and derivation

Hydrocarbon oxidations under NO_x-rich atmospheric conditions are sequences of reactions in which – follow-

ing the initial attack of a parent hydrocarbon by an oxidant, such as OH – reaction intermediates (alkyl, alkylperoxy and alkoxy radicals) interact with O_2 or NO to produce a carbonyl compound. These reactions are generally chain propagating. Depending on the nature of the hydrocarbon and/or the concentration level of atmospheric NO_x a fraction of these reactions may also be chain terminating to produce nitrites and/or nitrates. Moreover, unlike alkyl and alkylperoxy radicals, alkoxy radicals tend to be thermally unstable and are likely to decompose or isomerize whereupon new alkyl type radicals are formed and the reaction chain is re-started. An important question therefore is how such behaviour can be accounted for in lumped oxidation mechanisms. Such mechanisms are urgently needed in order to simplify the detailed mechanistic information in complex chemical-dynamical situations encountered e.g. in modelling of smog episodes.

As a useful descriptive tool of the net interaction of the oxidation chain of hydrocarbons with NO_x to generate NO_2 so called NOCON factors have been suggested [47,49]. The essence of this factor is to permit to condense detailed oxidation mechanisms of hydrocarbons in form of one single mechanistic equation of the form:

$$\mathrm{VOC} + \alpha\mathrm{NO} + \beta\mathrm{O_2} \rightarrow \gamma\mathrm{R'CHO} + \delta\mathrm{R'CH_2O}_x\mathrm{NO}_y + \varepsilon\mathrm{NO_2}$$

In here, the factor ε is the NOCON factor, i.e. the ratio of the number of moles of NO_2 formed per mol of hydrocarbons oxidized. The factors γ and δ reflect the total amount of the hydrocarbon which is oxidized to a carbonyl and which is transformed into chain terminating products such as nitrites ($x=1$, $y=1$) and nitrates ($x=1$, $y=2$), respectively. From mass balance considerations $\alpha = \delta + \varepsilon$. Although the above equation is the overall balance equation of a multitude of elementary reactions describing the oxidation of a hydrocarbon (as e.g. exemplified in the subsequent detailed mechanism of the oxidation of propane) this equation still describes the rate of the overall evolution of reagents and products provided all subsequent steps are fast compared to the initial rate of oxidation of the parent hydrocarbon. Accordingly the rate of NO_2 formation is given by the rate of the hydrocarbon oxidation reaction multiplied by the NOCON factor ε. For OH as the oxidant this rate then becomes:

$$\frac{\mathrm{d[NO_2]}}{\mathrm{d}t} = k_{\mathrm{OH}}[\mathrm{OH}][\mathrm{VOC}]\varepsilon$$

Equations of this type hold for all hydrocarbons present in an air mass including their oxygenated analogues, such as carbonyls, alcohols or acids. As a consequence, with the aid of NOCON factors the overall local rate of NO_2 formation in an air mass could be calculated simply on the basis of the composition, the concentration of the oxidant and the individual NOCON factors. However, because of the NO_x interactions with the hydrocarbon oxidation chain which lead to chain terminating products, NOCON factors are somewhat NO_x dependent.

In the present definition, NOCON factors are represented by the ratio:

$$\mathrm{NOCON} = \frac{[\mathrm{NO_2}]}{\Delta[\mathrm{VOC}]}$$

where the number of hydrocarbon molecules oxidized (Δ[VOC]) and the number of NO_2 molecules generated ($\Delta[NO_2]$) include all relevant processes of the mechanistic steps in VOC oxidation. Whilst the loss of VOC is normally only afforded in reaction with OH the formation of NO_2 in reaction of NO with the oxidation intermediates (RO_2 and HO_2) is in competition with the formation of nitrites and nitrates. Nevertheless, the amount of NO_2 produced can be measured directly in our laboratory experiment. The amount of hydrocarbon consumed (Δ[VOC]), however, is more difficult do determine.

To a first approximation, the amount of VOC oxidized may be taken as being equal to the concentration of radicals which initiate its oxidation. The basis of this approach is the notion that all oxidants present are exclusively consumed in reaction with the parent hydrocarbon which is present in large excess. In case of OH as a radical precursor, it is simple to calculate the amount of initially formed radicals from the parameters of the laser photolysis of its precursor H_2O_2 (laser pulse fluence, monochromatic absorption coefficient). However, this approach only provides a lower limit of Δ[VOC] since OH radicals are also regenerated in the course of the oxidation reaction. The time scale of this regeneration is comparable to the time scale of initial oxidant consumption. As a result, the amount of VOC oxidized is increased during the course of the reaction. The same applies to the amount of NO_2.

To correct for the effect of radical recycling on the consumption of VOC, we have chosen to use the OH integral $\int_0^\tau [\mathrm{OH}]\,\mathrm{d}t$as an equivalent measure for Δ[VOC]. As much as the OH concentration itself this integral can be measured with relatively high precision. As can be shown from a simple mathematical analysis of the OH radical profile, the product of this integral with the initial VOC concentration ($[\mathrm{VOC}]_0$) and the OH rate constant k_{OH} is equal to Δ[VOC].

The decay rate of OH for excess VOC is given by:

$$\frac{\mathrm{d[OH]}}{\mathrm{d}t} = -k_{\mathrm{OH}}[\mathrm{OH}][\mathrm{VOC}]_0$$

which upon integrations leads to:

$$[\mathrm{OH}]_\tau = [\mathrm{OH}]_0 \exp(-k_{\mathrm{OH}}[\mathrm{VOC}]_0\tau)$$

The time integral of the OH profile F, viz.

$$F = \int_0^t [\mathrm{OH}]_\tau \,\mathrm{d}\tau = [\mathrm{OH}]_0 \int_0^t \exp(-k_{\mathrm{OH}}[\mathrm{VOC}]_0\tau)\,\mathrm{d}\tau$$

is

$$F = [\mathrm{OH}]_0 \left\{ \frac{1}{-k_{\mathrm{OH}}[\mathrm{VOC}]_0} \exp(-k_{\mathrm{OH}}[\mathrm{VOC}]_0\tau) \right\} \Bigg|_0^t$$

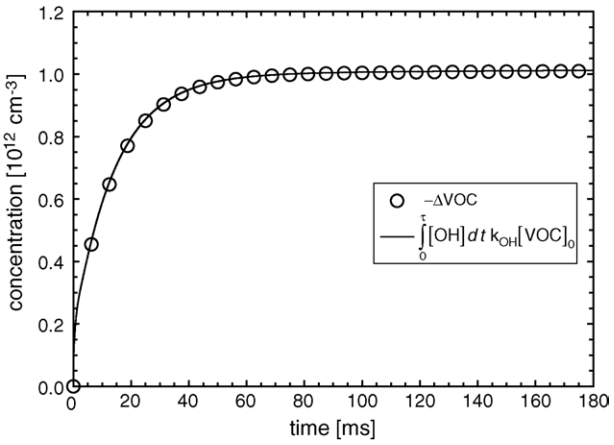

Fig. 2. Simulated Δ[propane] in comparison with the results from integration of simulated OH profiles for different reaction times.

For all reaction times ≥ 10 ms

$$F = [\mathrm{OH}]_0 \left\{ \frac{1}{k_{\mathrm{OH}}[\mathrm{VOC}]_0} \right\}$$

and hence

$$Fk_{\mathrm{OH}}[\mathrm{VOC}]_0 = [\mathrm{OH}]_0 \equiv \Delta[\mathrm{VOC}]$$

is a very satisfactory approximation.

In practice, the integration is performed by averaging over two adjacent data points of the time resolved OH profile and multiplying the result with time increment of the simulation or data acquisition. The sum of these values over a number of time increments corresponds to the OH integral for that reaction time. Fig. 2 demonstrates the correctness of this procedure by showing a comparison between integrated OH signals and Δ[propane] data, both obtained from simulation studies, for different reaction times. As can be seen, the agreement between the two is perfect over the entire time scale which lends confidence to the approach adopted. It should be emphasized, however, that the applicability of this approach to derive Δ[propane] data in real laboratory experiments requires high precision OH measurements at a very low concentration levels. We believe that this is the case with the present technique.

Fig. 2 also demonstrates that although the decay of the initial OH concentration occurs on the time scale of only a few ms the OH integral and hence the loss of VOC tend to grow up to at least 60 ms. Hence, the effective lifetime of OH in our experiment is roughly extended by a factor of 10 due to radical recycling.

3. Results and discussion

As has been mentioned above the present technique is of high versatility because the species monitored (OH and NO_2) are independent of the nature of the VOC. Nevertheless it needs to be validated using established oxidation mechanisms.

In the following we present results of integrated oxidation studies of propane as a model compound at $T = 298$ K. This compound has been chosen, because its oxidation mechanism is well understood and hence no larger errors are expected to be introduced by unknown reactions and/or unreliable rate coefficients. We will first present experimental observations of OH and NO_2 profiles and will then discuss the derivation of NOCON factors for this compound. Finally we will show how this factor is modified for different experimental conditions.

3.1. Experimental observations

The oxidation of propane has been studied using the laser pulse initiated generation of OH radicals in the presence of propane ($[\mathrm{propane}]_0 = 9.5 \times 10^{14}$ cm^{-3}) and NO ($[\mathrm{NO}]_0 = 2.0 \times 10^{13}$ to 1.2×10^{14} cm^{-3}). Hydrogen peroxide has been used as an OH precursor which was photolysed at 248 nm using the output of an excimer laser (Lambda Physics EMG 200). The total pressure has been chosen to be around 50 mbar.

Typical concentration profiles obtained for OH and NO_2 are presented in Fig. 3a–c. The different parts of this figure are for different initial NO concentrations but otherwise identical conditions. Whilst in each case, the initial decay of OH is of comparable rate (as shown by the individual inserts) the behaviour of OH at longer reaction times is very much dependent on the NO level. Whilst for $[\mathrm{NO}] = 2.0 \times 10^{13}$ cm^{-3} (Fig. 3a) there is substantial OH recycling producing even a secondary maximum in the OH concentration and a slow overall decay, this is not the case for high NO concentrations (i.e. 1.2×10^{14} cm^{-3}). In this case (Fig. 3c), the decay of OH is more monotonous and faster. Similar conclusions hold for the evolution of NO_2.

By a comparison between initial OH and final NO_2, Fig. 3 also demonstrates the extent of OH recycling. Although, in each of the cases presented the initial OH concentration was 3.2×10^{11} cm^{-3} the final NO_2 concentrations vary between 1×10^{12} and 3×10^{12} cm^{-3}, depending on the NO concentration. Hence, the average chain length of OH is in the order of 3.5–10 (see below).

In order to reproduce our experimental observations we have performed modelling calculations using the GEPASI software [51–53] for OH and NO_2 as well as other products from this reaction (see below) based on the mechanism outlined in Table 1 (see table below).This mechanism is a composite of all available reactions which deem essential in the oxidation of propane and the rate constants of which have been taken from a number of recent evaluations [26,29–32,54–56]. As can be seen from the comparison of measured and simulated profiles of Fig. 3 the agreement between the two is excellent. This agreement lends substantial support to the mechanistic and kinetic data base used as well as to the strength of the present technique to test such mechanisms.

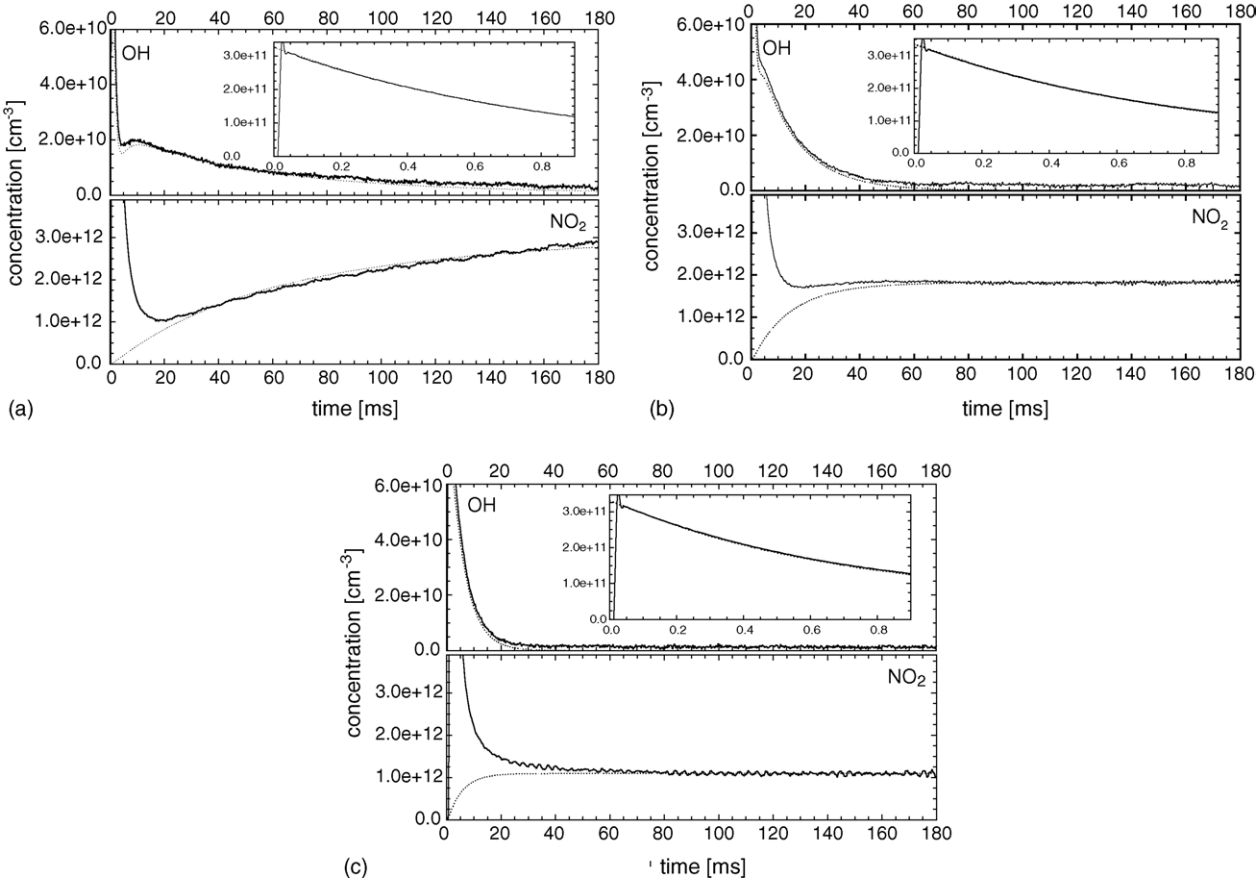

Fig. 3. Comparison between experimentally obtained (solid lines) and simulated (dotted lines) OH and NO_2 concentration–time profiles in the oxidation of propane The measured NO_2-concentration is corrected for diffusion (see text). Concentrations (in cm^{-3}): [propane] = 9.5×10^{14}; [H_2O_2] = 3.2×10^{13}; [O_2] = 1.1×10^{18}; [NO]: 2×10^{13} (a); 6×10^{13} (b); 1.2×10^{14} (c). The strong initial NO_2 signal is caused by stray light from the photolysis laser and is rejected in the analysis of the concentration profiles.

It should be emphasized that the modelling calculation contains no adjustable parameter, not even the initial OH concentration, and that henceforth we are presenting an oxidation experiment with very well controlled conditions at extremely low oxidant levels.

In order to characterise the extent of OH recycling in more detail we have performed additional model simulations in which the OH radicals generated each time the oxidation chain was completed were identified and labelled. The result from this simulation together with that for NO_2 are presented in Fig. 4.

As can be seen there is indeed considerable OH recycling during the course of the reaction. Simultaneously, the concentration of NO_2 builds up in successive chain cycles and only approaches a "final" value after about 45 ms, which corresponds to a total of >5 chain cycles. As a result of recycling the overall decay of OH is generally non-exponential or may even exhibit intermediate maxima depending on the choice of experimental conditions. One possibility to separate initial and recycled OH experimentally is the use of isotopic OD in the initialisation reaction. Such experiments are in progress and their results will be reported in a forthcoming publication [57].

The evolution of the other oxidation products (aldehydes, HNO_y and RNO_y), as obtained from the model simulation but not measured in this experiment, is shown in Fig. 5. The two parts (5a and b) are for the same experiment but for different time scales.

As is apparent from this figure, these stable products appear with a time constant similar to that of the formation of NO_2. Moreover, the main products of the oxidation of propane are the carbonyls acetone and propanal, the formation of which correspond to complete propane oxidation following either central or terminal attack of OH. Only a smaller fraction of the product distribution is from interactions of the oxidation chain with NO_x, forming notably propylnitrite and propylnitrate.

3.2. Measurements and model simulations of NOCON factors

As has been discussed above, NOCON factors are important quantities in characterising the extent of NO to NO_2

Table 1
Reactions and rate coefficients used for simulating the oxidation of propane

No.	Reaction	k (298 K)	A	n	E_A/R	Lit.
1	$OH + C_3H_8 \geq n\text{-}C_3H_7 + H_2O + \Delta VOC$	3.00E−13				[30] Web version, March 2005
2	$OH + C_3H_8 \geq i\text{-}C_3H_7 + H_2O + \Delta VOC$	8.00E−13				[30] Web version, March 2005
	Overall	1.10E−12	7.60E−12	0	585	[30] Web version, March 2005
3	$OH + HO_2 \geq O_2 + H_2O$	1.10E−10	4.80E−11	0	−250	[29]
4	$OH + NO \geq HONO$	7.34E−13	Termolecular see note[a]			[29]
5	$OH + HNO \geq H_2O + NO$	1.51E−11	8.00E−11	0	499	[55]
6	$OH + H_2O_2 \geq HO_2 + H_2O$	1.70E−12	2.90E−12	0	160	[29]
7	$OH + C_2H_5CHO \geq$ Prod1	2.00E−11	5.10E−12	0	−405	[30] Web version, March 2005
8	$OH +$ acetone $\geq CH_2C(O)CH_3 + H_2O$	1.70E−13	See note[b]			[30] Web version, March 2005
9	$OH + NO_2 \geq HONO_2$	1.75E−12	Termolecular see note[a]			[29]
10	$n\text{-}C_3H_7 + O_2 \geq n\text{-}C_3H_7O_2$	6.00E−12	6.00E−12	0	0	[30] Web version, March 2005
11	$i\text{-}C_3H_7 + O_2 \geq i\text{-}C_3H_7O_2$	1.10E−11	1.10E−11	0	0	[30] Web version, March 2005
12	$n\text{-}C_3H_7O_2 + NO \geq n\text{-}C_3H_7O + NO_2$	9.21E−12				[30] Web version, March 2005
13	$n\text{-}C_3H_7O_2 + NO \geq n\text{-}C_3H_7ONO_2$	1.88E−13				[30] Web version, March 2005
	Overall	9.40E−12	2.90E−12	0	−350	[30] Web version, March 2005
14	$n\text{-}C_3H_7O_2 + NO_2 \geq n\text{-}C_3H_7OONO_2$	5.65E−12	Not available			Estimated from [1]
15	$n\text{-}C_3H_7OONO_2 \geq n\text{-}C_3H_7O_2 + NO_2$	5.20	6.70E + 15	0	10368	Estimated from Ref. [26]
16	$i\text{-}C_3H_7O_2 + NO \geq i\text{-}C_3H_7ONO_2$	3.78E−13				[30] Web version, March 2005
17	$i\text{-}C_3H_7O_2 + NO \geq i\text{-}C_3H_7O + NO_2$	8.62E−12				[30] Web version, March 2005
	Overall	9.00E−12	2.70E−12	0	−360	[30] Web version, March 2005
18	$i\text{-}C_3H_7O_2 + NO_2 \geq i\text{-}C_3H_7OONO_2$	5.65E−12	Not available			[1]
19	$i\text{-}C_3H_7OONO_2 \geq i\text{-}C_3H_7O_2 + NO_2$	5.20	6.70E + 15	0	10368	[26]
20	$i\text{-}C_3H_7O + NO \geq i\text{-}C_3H_7ONO$	3.40E−11	Not available			[30] Web version, March 2005
21	$i\text{-}C_3H_7O + NO \geq$ acetone + HNO	6.50E−12	Not available			[30] Web version, March 2005
22	$n\text{-}C_3H_7O + NO \geq n\text{-}C_3H_7ONO$	3.80E−11	Not available			[30] Web version, March 2005
23	$n\text{-}C_3H_7O + O_2 \geq C_2H_5CHO + HO_2$	1.00E−14	2.60E−14	0	253	[30] Web version, March 2005
24	$n\text{-}C_3H_7O + NO_2 \geq n\text{-}C_3H_7ONO_2$	3.60E−11	Not available			[30] Web version, March 2005
25	$i\text{-}C_3H_7O + O_2 \geq$ acetone + HO_2	7.00E−15	1.90E−14	0	300	[30] Web version, March 2005
26	$i\text{-}C_3H_7O + NO_2 \geq i\text{-}C_3H_7ONO_2$	3.40E−11	3.40E−11	0	0	[36,31]
27	$NO_2 \geq$ Prod2	4.0	Not available			This work
28	$HO_2 + n\text{-}C_3H_7 \geq OH + n\text{-}C_3H_7O$	4.00E−11	Not available			[52]
29	$HO_2 + i\text{-}C3H_7 \geq CH_3CHO + CH_3 + OH$	4.00E−11	Not available			[52]
30	$HO_2 + HO_2 \geq H_2O_2 + O_2$	1.60E−12	2.20E−13	0	−600	[30] Web version, March 2005
31	$NO + HO_2 \geq NO_2 + OH$	8.80E−12	3.60E−12	0	−270	[30] Web version, March 2005
32	$n\text{-}C_3H_7O_2 + HO_2 \geq n\text{-}C_3H_7OOH + O_2$	1.19E−11	1.51E−13	0	−1300	[36,31]
33	$i\text{-}C_3H_7O_2 + HO_2 \geq i\text{-}C_3H_7OOH + O_2$	1.19E−11	1.51E−13	0	−1300	[36,31]
34	$OH \geq$ Prod3	10.0	Not available			This work

[a] Termolecular rates are calculated according to as described in Chapter 2.1 of source b.

Rate constants for termolecular reactions

Reaction	Low-pressure limit $k_0(T) = k_0^{300}(T/300)^{-n}$		High-pressure limit $k(T) = k^{300}(T/300)^{-m}$		Reference
	k_0^{300}	n	k^{300}	m	
$OH + NO \xrightarrow{M} HONO$	$7.0 \pm 1.0\ (-31)$	2.6 ± 0.3	$3.6 \pm 1.0\ (-11)$	0.1 ± 0.5	b
$OH + NO_2 \xrightarrow{M} HONO_2$	2.0 (−30)	3.0	2.5 (−11)	0	b

To obtain the effective second-order rate constant for a given condition of temperature and pressure (altitude), the following formula is used: $k_f([M], T) = \left(\frac{k_0(T)[M]}{1+\frac{k_0(T)[M]}{k_\infty(T)}}\right) 0.6^{\left\{1+\left[\log 10\left(\frac{k_0(T)[M]}{k_\infty(T)}\right)\right]^2\right\}^{-1}}$. The fixed value 0.6 that appears in this formula fits the data for all listed reactions adequately, although in principle this quantity may be different for each reaction, and also temperature dependent.

[b] Temperature dependence of acetone + OH (reaction (8)). 8.80E−12 exp(−1320/T) + 1.7E−14 exp(420/T) from Ref. [33] Web version March 2005.

conversion in the oxidation of VOCs in lumped oxidation mechanisms. Henceforth, it is of interest to demonstrate whether or not these quantities can directly be measured.

As we have already demonstrated our experiments permit the detailed monitoring of OH and NO_2 where the profiles observed for each of these species are in very satisfactory agreement with simulated profiles. However, due to the need to include NO in the reaction mixture there is also substantial recycling of the initial oxidant OH as well as chain termination. This must be taken into account when a characteristic quantity, such as a NOCON factor is determined.

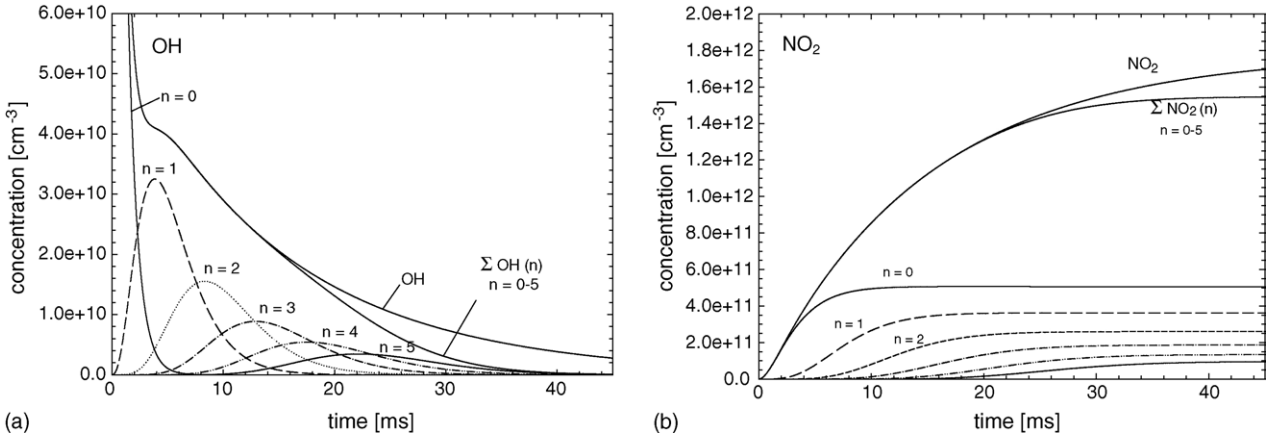

Fig. 4. Simulations of OH (a) and NO_2 (b) concentration/time profiles as specific for individual chain cycles ($n = 0$–5) in the pulse initiated oxidation of propane. The OH (NO_2) profile without index are those from the complete mechanism for infinite number of chain cycles. Concentrations (in cm^{-3}): $[OH]_0 = 3.2 \times 10^{11}$; $[propane]_0 = 9.4 \times 10^{14}$; $[O_2] = 1.1 \times 10^{18}$; $[NO] = 6 \times 10^{13}$; $[H_2O_2] = 3.1 \times 10^{13}$.

For the case of the OH induced oxidation of propane, the sequence of major oxidation reactions, is:

$$OH + C_3H_8 \rightarrow C_3H_7 + H_2O$$

$$C_3H_7 + O_2 + M \rightarrow C_3H_7O_2 + M$$

$$C_3H_7O_2 + NO \rightarrow C_3H_7O + NO_2$$

$$C_3H_7O + O_2 \rightarrow C_3H_6O(\text{acetone and propanal}) + HO_2$$

$$HO_2 + NO \rightarrow OH + NO_2$$

If we neglect the additional reactions in which alkoxy and alkylperoxy radicals interact with NO_x to form nitrites and nitrates in chain terminating reactions, the above sequence produces a theoretical NOCON factor of 2.0. This value is characteristic for simple oxidation chains in which there is only one RO_2 and one HO_2 interaction with NO to generate NO_2. Only for VOCs which in their oxidation mechanisms generate additional alkyl radicals through, i.e. isomerization and/or decomposition reactions of alkoxy radicals, viz:

$$RCH_2O + M \rightarrow R + CH_2O + M$$

the effective chain lengths are increased and NOCON factors larger than 2.0 will be produced. Unlike the effect of chain length the effect of chain termination tends to reduce the NOCON factor. This is because reactions such as:

$$RO_2 + NO(NO_2) \rightarrow RO_2NO(NO_2)$$

$$RO + NO(NO_2) \rightarrow RONO(NO_2)$$

are consumption processes of the VOC (and of NO) but there is no associated conversion to NO_2. In summary, therefore, NOCON factors (and their deviations from the standard value 2.0) provide valuable insight into the overall oxidation mechanisms with particular emphasis on net NO_2 formation.

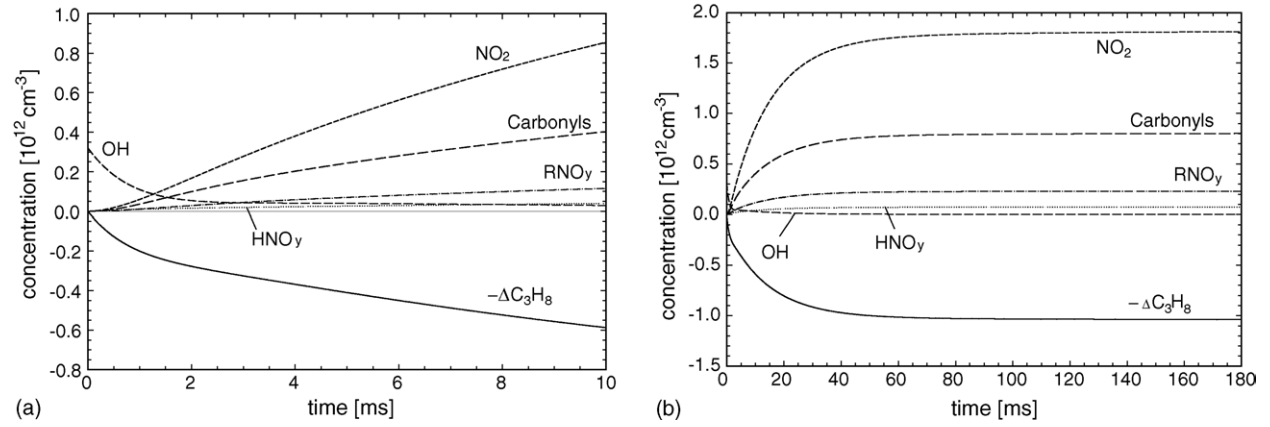

Fig. 5. Simulated evolution of the oxidation products in the oxidation of propane for different time scales ((a) $t = 10$ ms; (b) $t = 180$ ms). $-\Delta C_3H_8$ denotes the negative difference between $[C_3H_8]_0$ and $[C_3H_8]_t$. Carbonyls are the sum of C_2H_5CHO, acetone and CH_3CHO; HNO_y the sum of HNO, HONO and $HONO_2$; RNO_y the sum of *i*-C_3H_7ONO, *n*-C_3H_7ONO, *i*-$C_3H_7ONO_2$ and *n*-$C_3H_7ONO_2$. Concentrations (in cm^{-3}): $[OH]_0 = 3.2 \times 10^{11}$; $[C_3H_8]_0 = 9.4 \times 10^{14}$; $[NO]_0 = 6 \times 10^{13}$; $[H_2O_2]_0 = 3.1 \times 10^{13}$; $[O_2]_0 = 1.1 \times 10^{18}$.

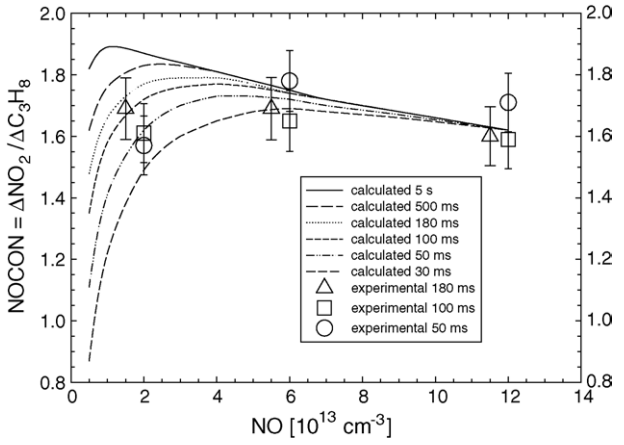

Fig. 6. Experimentally obtained NOCON factors for different NO concentrations and reaction times in comparison with calculated data. The experimental data for 180 ms (triangles) are displaced to slightly lower NO values for clarity.

Since both, chain length enhancement and chain termination are substance specific and [NO] dependent, respectively, NOCON factors cannot be universal. To determine substance specifity as well as the NO_x dependence is the aim of the current approach.

As has been elaborated above, the amount of NO_2 generated in the oxidation chain can be extracted directly from the measurements with sufficient confidence. The same is not true for the amount of propane oxidized, which cannot be determined experimentally. To circumvent this deficit of our technique, we have used the measurements of the OH profile for which the time integral is related to the concentration of propane consumed.

Measurements of NOCON factors as made from simultaneous observations of OH and NO_2 profiles are summarized in Fig. 6. The data shown are for different NO concentrations and for different overall reaction times. As can be seen, the data obtained are around 1.65 ± 0.1 with little dependence on these variables. The deviation from the 'theoretical' value 2.0 is ascribed to the extent of termination reactions involving NO_x.

In order to analyse these effects in more detail we have also performed corresponding modelling calculations in which from the simulated concentration profiles the values for $\Delta[NO_2]$ and Δ[propane] were extracted. The results of this calculation are equally presented in Fig. 6. This computational result demonstrates yet in more detail, the dependence of the NOCON factor on reaction time and NO concentration. As can be seen, the dependence on these variables is substantially stronger than demonstrated by the experimental data. This is because a substantial drop of the NOCON factor is simulated for low NO concentrations and short reaction times. Under these conditions, the peroxy + NO chemistry, which is responsible for the formation of NO_2, ceases. The dependence on reaction time which is mainly pronounced at low NO concentrations is attributed to a temporal delay between OH consumed and NO_2 formed.

In general, the experimental observations are in very satisfactory agreement with the results from the model simulations using a complete mechanisms. It should be emphasized that experiment and simulation contain no further adjustable parameter and therefore the agreement must be considered very gratifying.

4. Summary and outlook

In the present paper, we have demonstrated the feasibility of direct time resolved measurements of OH and NO_2 to study complex oxidation reactions. Moreover, in an application of this technique to the laser pulse initiated oxidation of propane by OH radicals it is demonstrated that experimental and simulated concentration profiles are in excellent agreement even at extremely low oxidant levels. On one hand, this agreement confirms the mechanistic and kinetic correctness of the oxidation process. On the other hand, it provides the possibility to identify and quantify unknown mechanistic steps and their rate coefficients. Therefore, we conclude that our experimental technique – albeit technically quite involved and not simple – will find very useful applications in further studies of VOC oxidation reactions.

A particular strength of our method is to test and quantify the extent of radical recycling. What has already become obvious, namely the detection of intermediate maxima in the OH profiles will become more pronounced if other oxidants, i.e. Cl atoms or isotopically labelled species, such as OD, are used in which case the generation of OH in the course of the reaction will be very pronounced. Previous applications of this method have already been demonstrated [48,57]. To clarify the role of radical recycling is an unresolved problem, for instance, in the oxidation of aromatics [58].

It has also been shown in this paper that NOCON factors are sensible definitions of NO_2 related informations of VOC oxidation mechanisms which can be measured within certain error limits by the current technique. NOCON factors are 2.0 for all simple oxidation sequences of VOCs in which there is no or little chain length extension or chain termination in parallel or subsequent reactions. Deviations from this value are indications of extended chain propagations and/or chain terminations which can be used for their identification and quantification. It should be additionally noted that although the NO_x concentrations used in our experiment are considerably larger than those encountered in the atmosphere, our experiments still simulate these conditions since the ratio of NO_x to oxidant are comparable in either case.

Acknowledgements

The initial parts of this work have been supported by BMBF within its tropospheric ozone research programme. Additional support by the EU project UTOPIHAN is also gratefully acknowledged.

References

[1] A.J. Haagen-Smit, C.E. Bradley, M.M. Fox, Ind. Eng. Chem. 45 (1953) 2086.
[2] P.A. Leighton, Photochemstry of Air Pollution, Academic Press, New York, 1961.
[3] B. Finlayson-Pitts, J. Pitts, Atmospheric Chemistry, Wiley, New York, 1986.
[4] R. Zellner, G. Weibring, Z. Phys. Chem. 161 (1989) 167.
[5] M. Kanakidou, H.B. Singh, K.M. Valentin, P.J. Crutzen, J. Geophys. Res. 96 (1991) 15395–15413.
[6] Y. Wang, D.J. Jacob, J.A. Logan, J. Geophys. Res. 103 (1998) 10757–10767.
[7] P.O. Wennberg, et al., Science 279 (1998) 49–53.
[8] S. Houweling, F. Dentener, J. Lelieveld, J. Geophys. Res. 103 (1998) 10673–10696.
[9] J.F. Müller, G. Brasseur, J. Geophys. Res. 104 (1999) 1705–1715.
[10] N. Poisson, M. Kanakidou, P.J. Crutzen, J. Atmos. Chem. 35 (2000) 157–230.
[11] H. Niki, P.D. Maker, C.M. Savage, L.P. Breitenbach, J. Phys. Chem. 85 (1981) 877–881.
[12] R. Atkinson, S.M. Aschmann, J. Arey, Environ. Sci. Technol. 26 (1992) 1397–1403.
[13] J. Arey, S.M. Aschmann, E.S.C. Kwok, R. Atkinson, J. Phys. Chem. A 105 (2001) 1020–1027.
[14] F. Cavalli, H. Geiger, I. Barnes, K.H. Becker, Environ. Sci. Technol. 36 (2001) 1263–1270.
[15] I.W.M. Smith, R. Zellner, J. Chem. Soc. Faraday II 69 (1973) 1617.
[16] R. Zellner, K. Lorenz, J. Phys. Chem. 88 (1984) 984.
[17] J.G. Anderson, J. Geophys. Res. 76 (1971) 4634–4652.
[18] N.M. Donahue, J.H. Kroll, J.G. Anderson, Geophys. Res. Lett. 25 (1998) 59–62.
[19] F. Holland, M. Hessling, A. Hofzumahaus, J. Atmos. Sci. 52 (1995) 3393–3401.
[20] K. Lorenz, D. Rhäsa, B. Fritz, R. Zellner, Ber. Bunsenges. Phys. Chem. 89 (1985) 341–342.
[21] C. Mund, C. Fockenberg, R. Zellner, Ber. Bunsenges. Phys. Chem. 102 (1998) 709–715.
[22] C. Fittschen, A. Frenzel, K. Imrik, P. Devolder, Int. J. Chem. Kinet. 31 (1999).
[23] Ch. Lotz, R. Zellner, Phys. Chem. Chem. Phys. 2 (2000) 2553–2560.
[24] W. Deng, Ch. Wang, D.R. Katz, G.R. Gawinski, A.J. Davis, Th.S. Dibble, Chem. Phys. Lett. 330 (2000) 541–546.
[25] W. Deng, A.J. Davis, L. Zhang, D.R. Katz, Th.S. Dibble, J. Phys. Chem A 105 (2001) 8985–8990.
[26] P.D. Lightfoot, R.A. Cox, J.N. Crowley, M. Destriau, G.D. Hayman, M.E. Jenkin, G.K. Moortgat, F. Zabel, Atmos. Environ. 26A (1992) 1805–1961.
[27] C.A. Taatjes, D.B. Oh, Appl. Opt. 36 (1997) 5817.
[28] R. Atkinson, Int. J. Chem. Kinet. 9 (1997) 99–111.
[29] S.P. Sander, R.R. Friedel, D.M. Golden, M.J. Kurylo, R.E. Huie, V.L. Orkin, G.K. Moortgat, A.R. Ravishankara, C.E. Kolb, M.J. Molina, B.J. Finlayson-Pitts, Chemical Kinetics and Photochemical Data for Use in Atmospheric Studies No. 14, JPL Publication 02-25, 2003.
[30] R. Atkinson, D.L. Baulch, R.A. Cox, J.N. Crowley, R.F. Hampson, R.G. Hynes, M.E. Jenkin, J.A. Kerr, M.J. Rossi, J. Troe, Summary of Evaluated Kinetic and Photochemical Data for Atmospheric Chemistry—Iupac Subcommittee on Gas Kinetic Data Evaluation for Atmospheric Chemistry: Web Version March 2005. http://www.iupac-kinetic.ch.cam.ac.uk.
[31] S.M. Saunders, M.E. Jenkin, R.G. Derwent, M.J. Pilling, Atmos. Chem. Phys. 3 (2003) 161–180.
[32] M.E. Jenkin, S.M. Saunders, V. Wagner, M.J. Pilling, Atmos. Chem. Phys. 3 (2003) 181–193.
[33] R. Atkinson, E.S.C. Kwok, Atmos. Environ. 14 (1995) 1685–1695.
[34] R. Atkinson, J. Phys. Chem. Ref. Data 2 (1997) 215–290.
[35] H. Somnitz, R. Zellner, Phys. Chem. Chem. Phys. 2 (2000) 1899–1905.
[36] H. Somnitz, R. Zellner, Phys. Chem. Chem. Phys. 2 (2000) 1907–1918.
[37] H. Somnitz, R. Zellner, Phys. Chem. Chem. Phys. 2 (2000) 4319–4325.
[38] B.F. Magnussen, B.H. Hjertager, Proceedings of the 16th International Syymposium on Combustion, The Combustion Institute, 1976.
[39] B. Kärcher, J. Geophys. Res. 102 (1997) 19119–19135.
[40] G. Gleitsmann, R. Zellner, Phys. Chem. Chem. Phys. 1 (1999) 5503–5509.
[41] C. Kuhr, S. Staus, A. Schönbucher, Prog. Comp. Fluid Dynam. 3 (2003) 151.
[42a] D.S. McKenna, P. Konopka, J.-U. Grooß, G. Günther, R. Müller, R. Spang, D. Offermann, Y. Orsolini, J. Geophys. Res. 107 (2002) 4309–4324.
[42b] D.S. McKenna, P. Konopka, J.-U. Grooß, G. Günther, R. Müller, R. Spang, D. Offermann, Y. Orsolini, J. Geophys. Res. 107 (2002) 4256–4270.
[43] W.R. Stockwell, P. Middleton, J.S. Chang, X. Tang, J. Geophys. Res. 95 (1990) 16343–16367.
[44] W.R. Stockwell, F. Kirchner, M. Kuhn, J. Geophys. Res. 102 (1997) 25847–25879.
[45] A. Hoffmann, V. Mörs, R. Zellner, Ber. Bunsenges. Phys. Chem. 96 (1992) 437–440.
[46] V. Mörs, A. Hoffmann, W. Malms, H. Hein, R. Zellner, EUROTRAC Symposium Proceedings, vol. 2, 1996, pp. 571–575.
[47] H. Hein, A. Hoffmann, R. Zellner, Ber. Bunsenges. Phys. Chem. 102 (1998) 1840–1849.
[48a] H. Hein, A. Hoffmann, R. Zellner, Phys. Chem. Chem. Phys. 1 (1999) 3743–3752.
[48b] H. Hein, PhD Thesis, Essen, 1999.
[49] H. Hein, H. Somnitz, A. Hoffmann, R. Zellner, Z. Physikal. Chem. 214 (2000) 449–471.
[50] A. Hoffmann, PhD Thesis, Göttingen, 1991.
[51] P. Mendes, Comput. Appl. Biosci. 9 (1993) 563–571.
[52] P. Mendes, Trends Biochem. Sci. 22 (1997) 361–363.
[53] P. Mendes, D.B. Kell, Bioinformatics 14 (1998) 869–883.
[54] H. Adachi, N. Basco, Int. J. Chem. Kinet. 14 (1982) 1243–1251.
[55] W. Tsang, J. Phys. Chem. Ref. Data 17 (1988) 887–952.
[56] W. Tsang, J.T. Herron, J. Phys. Chem. Ref. Data 20 (1991) 609–663.
[57] J. Grossmann, A. Hoffmann, R. Zellner, in press.
[58] J.G. Calvert, R. Atkinson, K.H. Becker, R.M. Kamens, J.H. Seinfeld, T.H. Wallington, G. Yarwood, The Mechanisms of Atmospheric Oxidation of the Aromatic Hydrocarbons, 2001.